

Packing systematics of the silica polymorphs: The role played by O-O nonbonded interactions in the compression of quartz

RICHARD M. THOMPSON* AND ROBERT T. DOWNS

Department of Geosciences, University of Arizona, Tucson, Arizona 85721-0077, U.S.A.

ABSTRACT

The anion skeleton of quartz is a distorted body-centered cubic (BCC) arrangement. A hypothetical ideal BCC crystal structure for quartz has been derived and used to locate and describe the unoccupied tetrahedral sites, quantify the distortion of the quartz anion arrangement from ideal BCC, and characterize the role of tetrahedral distortion and O-O interactions in the compression of quartz. Quartz has eight crystallographically nonequivalent tetrahedra, one occupied by silicon and seven unoccupied. These tetrahedra completely fill space, something that cannot be done using only regular tetrahedra. In ideal BCC quartz, the nonequivalent tetrahedra are identical in size and shape with a unique geometry and are referred to as Sommerville tetrahedra. In reality, the unoccupied tetrahedra of quartz are very distorted from both regular and Sommerville tetrahedra. Changes in the unoccupied tetrahedra are responsible for most of the compression in quartz with pressure, as the volume of the Si tetrahedron decreases by <1% over 10.2 GPa, but the volume of the bulk structure decreases by almost 16%. The ideal BCC quartz has been used to quantify the distortion from ideal BCC of the O arrangement in quartz at several pressures up to 10.2 GPa. Distortion decreases by over 60% across this domain. Other parameters have been derived to quantify the distortion of the unoccupied and occupied tetrahedra in quartz from Sommerville tetrahedra, the characteristic tetrahedra of BCC. By all measures, the anion packing in quartz approaches ideal BCC as pressure increases. The compression mechanisms of quartz are compared to those of cristobalite and coesite. Si-O-Si angle-bending controls compression in each of these minerals. The bulk moduli of these minerals are shown to correlate with average nearest inter-tetrahedral anion distances, consistent with the hypothesis that anion-anion interactions stiffen the Si-O-Si angle as inter-tetrahedral anion distances decrease. The tetrahedral distortion in quartz with pressure is attributed to anion-anion interaction, and is not considered a compression mechanism.

Keywords: Quartz, high pressure, body-centered cubic, packing

INTRODUCTION

Quartz is an important Earth material that may constitute approximately 20% of the upper continental crust (Taylor and McLennan 1985). The simple chemistry and well-characterized structure of this mineral make it an excellent material to experiment on and theorize about, and the results can provide valuable insight into more complex materials. Quartz is composed solely of corner-sharing SiO₄ silica tetrahedra, a primary building block of many of the Earth's crustal and mantle minerals, lunar and martian minerals, and meteoritic minerals (Deer et al. 1978). Quartz is therefore an outstanding model material for investigating the response of this fundamental structural unit to changes in *P*, *T*, and *x*. These facts have spawned a vast literature of experimental and theoretical studies of quartz at ambient and non-ambient conditions. Investigations into the behavior of quartz at high pressure have revealed an anomalous distortion in the silica tetrahedra with pressure not typically seen in other silicates. The present study is motivated by the desire to understand the unusual changes in the silicate tetrahedra of quartz with pressure.

Jorgensen (1978) conducted the first high-pressure structure refinements on quartz using data collected by powder neutron

diffraction to 2.8 GPa. He listed three possible compression mechanisms: Si-O-Si angle-bending, tetrahedral distortion, and Si-O bond compression, concluding that Si-O-Si angle-bending makes the greatest contribution to the compression of quartz, tetrahedral distortion is also important, but the effect of bond compression is minimal. d'Amour et al. (1979) reported the first structure refinements from single-crystal X-ray diffraction. Reaching pressures of 6.8 GPa, they concluded that the observed compression could be accounted for by Si-O-Si angle-bending alone. Levien et al. (1980) compressed quartz to 6.1 GPa, collecting much more precise data than the earlier studies. In addition to angle-bending, they determined that there was a small component of bond compression, the magnitude of which lay within the error of the less precise earlier studies, and they verified the tetrahedral distortion mechanism of Jorgensen (1978). They further noted that the rate of change of distortion increased with pressure, making this mechanism more important at higher pressures. Ogata et al. (1987) saw similar trends at simultaneous high pressure and temperature. Hazen et al. (1989) compressed quartz to 15.3 GPa, interpreting irreversible crystal degradation as evidence of amorphization at the highest pressure. Discounting the role of bond compression in quartz, they attributed all volume decrease to angle-bending. They observed extreme distortion of the tetrahedra, but did not consider

* E-mail: rmthomps@email.arizona.edu

this to be a compression mechanism. They also suggested that the O atoms were moving toward a close-packed arrangement with pressure. Glinnemann et al. (1992) undertook a study of the compression of quartz to 10.2 GPa, reiterating the view that quartz is compressed mainly through angle-bending, with a smaller contribution from tetrahedral distortion. Kim-Zajonc et al. (1999) extended these structural observations to 13.1 GPa. Continuing diffraction up to 19.3 GPa did not produce evidence of amorphization. Compression of quartz and its homeotypes beyond 20 GPa by several investigators has produced evidence of amorphization and/or novel phase transitions (cf. Haines et al. 2001 and references therein).

Sowa (1988) attributed the distortion of the tetrahedra in quartz with pressure to the movement of the anions toward body-centered cubic (BCC) packing. She calculated Dirichlet domains for the anions in quartz and realized that these domains were distorted cuboctahedra (perfect cuboctahedra result from ideal BCC packing), and that these cuboctahedra became less distorted with pressure. The Dirichlet domain for a given anion is the region of space containing every point that is closer to the given anion than to any other. The boundaries of the domain are equidistant between two anions. Sowa (1988) characterized the O packing of quartz and its changes with pressure, but did not relate her observations to O-O interactions or any other forcing mechanism.

Traditionally, crystal chemistry has considered the analysis of anion-cation interactions to be the key to understanding the changes in crystal structure with pressure, temperature, and changes in composition (Pauling 1940; Bragg et al. 1965; Hazen and Finger 1982). Crystal structures typically are compressed or expanded by “first-order” mechanisms that include inter-polyhedral angle-bending of cation-anion-cation angles (e.g., Si-O-Si bending in quartz), cation-anion bond compression (e.g., the Mg-O bond in MgO), intermolecular distance changes (e.g., in a layer structure such as graphite; Hazen 1999), and phase transitions. Additionally, Hazen (1999) identified the following mechanisms as being of lesser significance but still important: polyhedral distortion, cation order-disorder reactions, electronic transitions, and second-nearest neighbor cation-cation interactions.

However, theoretical work shows that anion-anion interactions play an important role in crystal chemistry (cf. Cohen 1994; Prencipe and Nestola 2007). Most work on the geometry of anion arrangements in minerals is descriptive, i.e., identifying and classifying the packing schemes of the anions (cf. O’Keefe and Hyde 1996). Packing indices have been derived by several investigators to quantify the distortion of anion arrangements and their response to changes in P , T , and x (cf. Thompson and Downs 2001a). We have worked extensively on actual and hypothetical packings in pyroxenes (Thompson and Downs 2001a, 2001b, 2003, 2004, 2008; Origlieri et al. 2003; Thompson et al. 2005; McCarthy et al. 2008; Nestola et al. 2008). However, it is difficult to unambiguously ascribe pressure-induced changes in either packing or polyhedral distortion in many minerals, including pyroxenes, to anion-anion interaction because many of the minerals whose packing arrangements have been described are based on distorted closest-packing of anions. In closest-packed structures, both anion-anion repulsion and volume reduction have the same effect of decreasing both packing and polyhedral distortion because tetrahedra and octahedra in ideal closest-

packing are perfectly regular. Despite this, Thompson and Downs (2008) used geometric models to derive evidence of anion-anion interaction in diopside.

Using the conclusion of Sowa (1988), that quartz has a distorted BCC anion skeleton, as a starting point, in this paper we will derive and present some new crystallographic data on quartz including data sets for hypothetical ideal BCC quartz and the locations of all of the unoccupied tetrahedral voids in quartz, quantify the distortion of the quartz anion arrangement from ideal BCC, and characterize the role of tetrahedral distortion and O-O interactions in the compression of quartz. Because quartz is based on BCC packing of anions and the tetrahedra in ideal BCC have a distinctive non-regular geometry, it is possible to distinguish between the effects of anion-anion interaction and volume reduction in quartz, in contrast to minerals based on closest-packing of anions. In quartz, the need to reduce volume with pressure would tend to make the tetrahedra more regular, but anion-anion repulsion would make them more like the distinctive tetrahedra of ideal BCC. Here we define “compression mechanism” as an atomic behavior that reduces the volume of a crystal as pressure increases. This narrow definition is chosen to distinguish between atomic behaviors that reduce volume in response to increasing pressure and those that reflect other intracrystal processes such as electrostatic repulsion. The net atomic behavior of a crystal under increasing pressure is the result of competing forces, and we are attempting to isolate which forces are responsible for various observed atomic behaviors, to move from observation to explanation. For instance, it is clear that Si-O-Si angle-bending is a mechanism that reduces the volume of quartz as pressure increases and is therefore a compression mechanism by our definition. We will provide evidence that increasing tetrahedral distortion in quartz with pressure arises from anion-anion interaction and stiffens the structure, and therefore by our definition, should not be classified as a compression mechanism, but should be characterized in a manner that reflects the process that causes the distortion. If Si-O-Si angle-bending is called a “compression mechanism” because it reduces cell volume of the crystal under pressure, tetrahedral distortion might be called an “anion distancing mechanism” because it maximizes the shortest nearest neighbor O-O distance as pressure increases. There is no a priori reason to assume that Si-O-Si angle-bending will necessarily distort the silica tetrahedra in quartz. Rigid unit mode, RUM, analysis has demonstrated the existence of RUMs in quartz that allow Si-O-Si bending without tetrahedral distortion (cf. Ross 2000 and references therein).

Because this paper is concerned with drawing conclusions about anion-anion interactions in quartz under pressure, we are specifically reporting about α -quartz and all instances of the word “quartz” could be replaced with “ α -quartz” without changing our meaning. However, β -quartz is displacively related to α -quartz, is also based on BCC packing of anions, and could also be analyzed using the mathematical tools presented in this paper.

FUNDAMENTALS OF BCC PACKING AND QUARTZ

Space cannot be completely filled by regular tetrahedra, but ideal BCC packing completely fills space with congruent (i.e., identical in size and shape) tetrahedra that are not regular (Table 1, Fig. 1) (Sommerville 1923a, 1923b). O’Keefe and Hyde

(1996) named these distinctive tetrahedra after D.M.Y. Sommerville, a mathematician who worked on the problem of space-filling tetrahedra (1923a, 1923b). Figure 1 shows two views of a Sommerville tetrahedron chosen to highlight its unusual geometry. Table 1 is a comparison between a regular tetrahedron and a Sommerville tetrahedron. It also contains Cartesian coordinates for the two tetrahedral types so that the reader can easily create data files for crystal-drawing programs to make a more extensive visual examination. Each face of a Sommerville tetrahedron is an isosceles triangle with the long edge 15% longer than the short edges and an opposing angle of $\cos^{-1}(1/3) \approx 70.53^\circ$. This gives the tetrahedron two different dihedral (interfacial) angle values, 90 and 45° . A Sommerville tetrahedron has a 10% greater volume and a 6% longer centroid-vertex separation (i.e., bond length) than a regular tetrahedron with an edge length equal to the shortest Sommerville edge. Assuming that the shortest edge in a tetrahedron represents a limiting O-O distance at a given pressure, this means that regular tetrahedra are more volume efficient than Sommerville tetrahedra. This does not prove that the most efficient way to reduce volume in the bulk quartz crystal is to make the SiO_4 tetrahedra more regular, but it is consistent with an alternative explanation for the increasing tetrahedral distortion in quartz with pressure.

Each sphere in an ideal BCC arrangement is at the vertex of 24 Sommerville tetrahedra, so each tetrahedron contains 1/24 of a sphere per vertex (Fig. 1), for a total 1/6 sphere per tetrahedron. Therefore, an ideal BCC arrangement of equal-sized spheres has six tetrahedral sites for each sphere. The BCC unit cell contains two spheres (one at the center and 1/8 sphere at each of the eight corners of the cube) and therefore 12 tetrahedral sites. The unit cell of quartz comprises three unit cells of BCC, so there are 36 tetrahedral sites in the unit cell of quartz, of which three are occupied by silicon and the rest are unoccupied. These 36 sites are divided into eight crystallographically non-equivalent sites in the symmetry of quartz, space group $P3_121$. Table 2 lists the positions of these sites, with the unoccupied sites denoted V for void, and their multiplicities: $3 \times \text{Si} + 3 \times \text{V1} + 3 \times \text{V2} + 3 \times \text{V3} + 6 \times \text{V4} + 6 \times \text{V5} + 6 \times \text{V6} + 6 \times \text{V7} = 36$ T sites. Figure 2 shows four views of quartz along $[210]$: quartz at 0 and 10.2 GPa, ideal BCC quartz, and the largest of the seven unoccupied symmetrically nonequivalent tetrahedral sites (V1 in Table 2) in 0 GPa quartz with the silica tetrahedra rendered invisible. Data for quartz at 0 and 10.2 GPa used to make Figure 2 are from Glinnemann et al. (1992). Table 2 contains the complete structural

data for the ideal BCC quartz, with data collected from a synthetic quartz sample included for comparison (Glinnemann et al. 1992). Figure 3 illustrates the relationship between the BCC unit cell and unit cell of quartz. The figure compares the perfect BCC cell of ideal BCC quartz with the distorted BCC cell of a synthetic quartz sample (Glinnemann et al. 1992). The coordinates of the corners of the perfect BCC cube are compared with those of synthetic quartz in Table 3. The faces of the perfect BCC cube are parallel to the planes $(\bar{1}\bar{1}1)$, (011) , and $(10\bar{1})$ in ideal quartz. In ideal BCC quartz, each of the eight non-equivalent tetrahedra

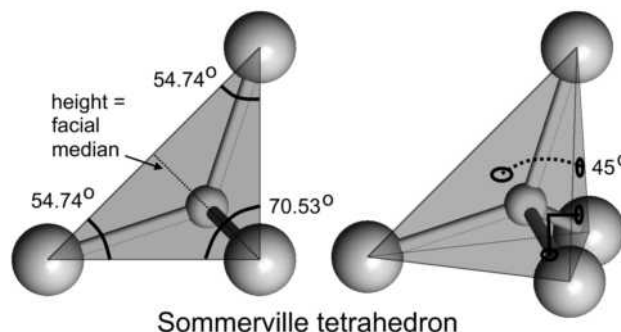


FIGURE 1. Two views of a Sommerville tetrahedron (O'Keeffe and Hyde 1996) chosen to highlight its unusual geometry.

TABLE 2. Structural data for ideal BCC quartz

Atom	Multiplicity	Ideal BCC			$P = 0$ GPa		
		x	y	z	x	y	z
Si	3	5/12	0	0	0.4698	0	0
V1	3	5/12	0	1/2	0.3593	0	1/2
V2	3	11/12	0	0	0.9700	0	0
V3	3	11/12	0	1/2	0.8593	0	1/2
V4	6	1/12	1/3	1/6	0.1407	0.3907	1/6
V5*	6	7/12	1/3	1/6	0.6407	0.3907	1/6
V6	6	1/4	2/3	1/3	1/4	0.7200	1/3
V7	6	3/4	2/3	1/3	3/4	0.7200	1/3
O	6	1/3	1/3	-1/12	0.4151	0.2675	-0.1194

Notes: Ideal BCC quartz is a hypothetical crystal with space group $P3_121$, origin shift $[0\ 0\ 1/3]$. For model O radius r , $a = 4\sqrt{6}r/3$, $c = 4r$, $c/a = \sqrt{3}/2$. V sites are tetrahedral sites that are unoccupied in quartz (tetrahedral voids). The $P3_121$ enantiomorph with origin shift $[0\ 0\ 2/3]$ in the Levien and Prewitt (1980) setting can be derived from this data by reversing the sign of each atom's z coordinate. Values for a synthetic quartz sample at room conditions from Glinnemann et al. (1992) have been included for comparison. V sites in synthetic quartz are the centroids of the unoccupied tetrahedral sites. *V5 in ambient condition quartz is so distorted that the four nearest O atoms to the centroid do not form the correct tetrahedron. Use (0.6,0.35,0.15) in a crystal-drawing program.

TABLE 1. A statistical comparison between a regular tetrahedron and a Sommerville tetrahedron

	Regular		Sommerville		Exact expressions with edge = 2r	
		no.		no.	Regular	Sommerville
Edge length	2	6	2, 2.31	4, 2	2r	$2r, (4/\sqrt{3})r$
Tetrahedral angles	109.47°	6	101.54°, 126.87°	4, 2	$\cos^{-1}(-1/3)$	$\cos^{-1}(-1/5), \cos^{-1}(-3/5)$
Dihedral angles	70.53°	6	45°, 90°	4, 2	$\cos^{-1}(1/3)$	$\cos^{-1}(\sqrt{2}/2), \cos^{-1}(0)$
Intrafacial angles	60°	12	54.74°, 70.53°	8, 4	$\cos^{-1}(1/2)$	$\cos^{-1}(1/\sqrt{3}), \cos^{-1}(1/3)$
Facial median	1.73	3	1.63	1	$\sqrt{3}r$	$(4/\sqrt{6})r$
Height, h	1.63		1.63		$(4/\sqrt{6})r$	$(4/\sqrt{6})r$
Volume	0.94		1.03		$\sqrt{(8/9)}r^3$	$(16/9\sqrt{3})r^3$
Centroid height	0.41		0.41		h/4	h/4
R(centroid-vertex)	1.22		1.29		$(3/\sqrt{6})r$	$\sqrt{(5/3)}r$
Cartesian coordinates	(0,0,0) (2r,0,0) ($r, \sqrt{3}r, 0$) ($r, \sqrt{3}r/3, 4r/\sqrt{6}$)		(0,0,0) ($4r/\sqrt{3}, 0, 0$) ($2r/\sqrt{3}, 4r/\sqrt{6}, 0$) ($2r/\sqrt{3}, 0, 4r/\sqrt{6}$)			
Centroid		$(r, \sqrt{3}r/3, r/\sqrt{6})$		$(2r/\sqrt{3}, r/\sqrt{6}, r/\sqrt{6})$		

Note: Exact expressions are parameterized in terms of a hypothetical model O radius = r.

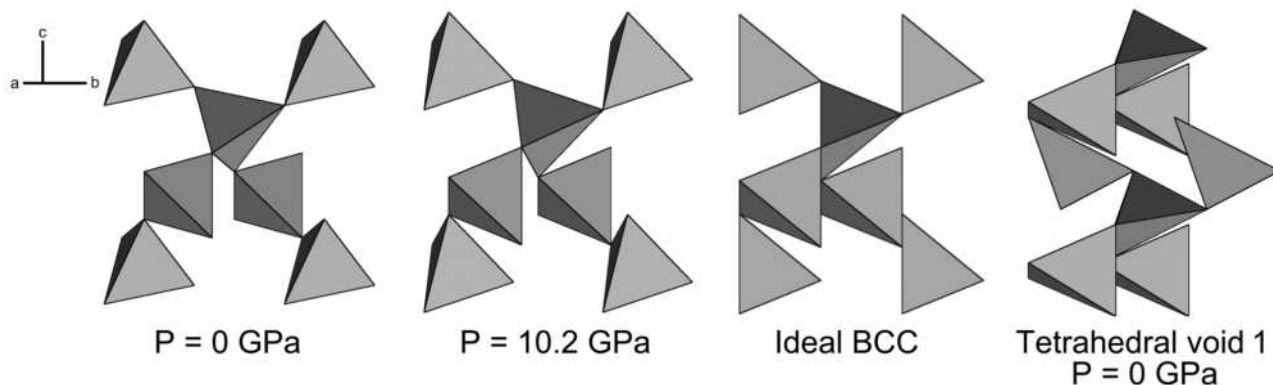


FIGURE 2. Four views of quartz down [210]. Data for quartz at 0 and 10.2 GPa are from Glinnemann et al. (1992).

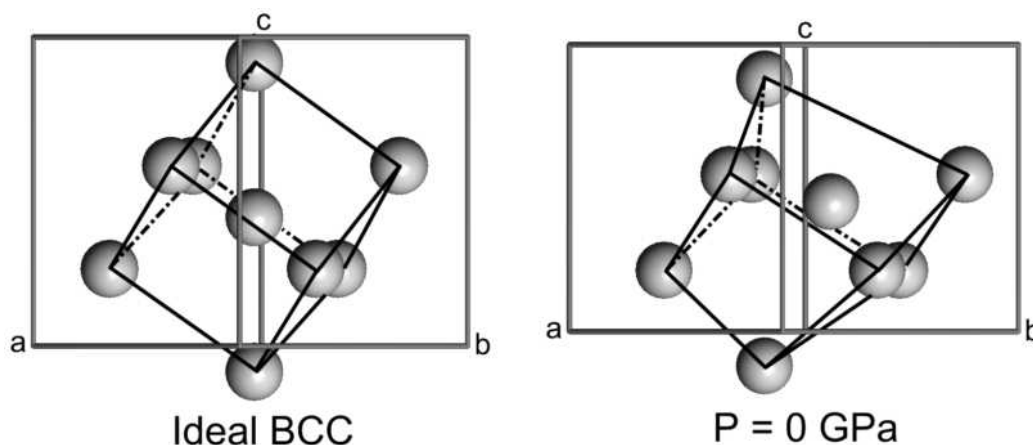


FIGURE 3. The relationship between the BCC unit cell and the quartz unit cell. A comparison between the perfect BCC unit cell in hypothetical ideal BCC quartz and the distorted BCC unit cell in a synthetic quartz sample (Glinnemann et al. 1992).

(in quartz symmetry) are perfect Sommerville tetrahedra of the same size and shape, but are not equivalent under the operators of the space group of quartz, $P3_121$. As the O skeleton of a natural or synthetic quartz sample gets closer to ideal BCC with pressure, the tetrahedra should become less regular, and more like Sommerville tetrahedra. These observations will be used to quantify the changes in the packing arrangement of quartz with pressure in several ways in the next section.

RESPONSE OF THE OXIDE ANION ARRAY IN QUARTZ TO PRESSURE

To look at the change in the bulk O arrangement of quartz with pressure, a parameter, U_{BCC} , has been derived that quantifies the distortion of the anion skeleton of quartz from ideal BCC. It is a measure of the mean squared displacement, i.e., variance, of 600 observed anions (a $5 \times 5 \times 4$ block of unit cells) from their ideal equivalents: $U_{\text{BCC}} = \sum_{i=1,600} [R_i^2(\text{observed-ideal})/600]$, where R_i is the distance from the i^{th} observed anion to its ideal equivalent. The fit between the observed and ideal arrangements is accomplished by rotating the ideal arrangement and varying its model O radius (i.e., the radius of the equal-sized spheres in the ideal BCC arrangement) until U_{BCC} is minimized. A U_{BCC} value of zero is perfectly BCC. A value of one is very distorted, so distortion from BCC increases as U_{BCC} increases. Alternatively, one can think of packing efficiency as increasing as U_{BCC} decreases. A similar parameter for cubic-closest packing and hexagonal closest-packing is described in detail in Thompson and Downs (2001a).

TABLE 3. Coordinates of O atoms in quartz that form a BCC unit cell

Ideal BCC			P = 0 GPa		
x	y	z	x	y	z
1/3	1/3	11/12	0.4151	0.2675	0.8806
0	2/3	7/12	-0.1476	0.5849	0.54727
-1/3	0	1/4	0.2675	0.1476	0.2193
2/3	1	1/4	0.7325	1.1476	0.2193
1/3	1/3	-1/12	0.4151	0.2675	-0.1194
2/3	0	1/4	0.7325	0.1476	0.2193
1	2/3	7/12	0.8524	0.5849	0.54727
0	-1/3	7/12	-0.1476	-0.4151	0.54727
Central sphere			Central atom		
x	y	z	x	y	z
1/3	1/3	5/12	0.2675	0.4151	0.45273

Notes: The coordinates of the corners of the perfect BCC unit cell of hypothetical ideal BCC quartz and of the distorted BCC unit cell in a synthetic quartz sample (Glinnemann et al. 1992).

Figure 4 is a plot of U_{BCC} vs. pressure for a synthetic quartz sample (Glinnemann et al. 1992). U_{BCC} decreases from 0.72 to 0.28 over 10.2 GPa. The fitted quadratic in Figure 4 reaches its minimum value of 0.1 \AA^2 at 14 GPa, suggesting that forces within quartz may prevent it from ever becoming perfectly BCC as pressure increases, and that quartz must alter its compression pathway as pressure reaches and exceeds ~ 14 GPa. The rate of decrease of U_{BCC} with pressure is two to three times greater than any of the analogous distortion parameter values reported for the pyroxenes, olivines, and other M_2SiO_4 polymorphs, and various other minerals examined by Thompson and Downs (2008) and references therein. The BCC packing efficiency of quartz dramatically improves with pressure. This necessarily means that the

tetrahedra in quartz become more like Sommerville tetrahedra.

To look at the change of the individual tetrahedra, unoccupied or occupied, in quartz with pressure, the intrafacial angle variance was calculated for all of the tetrahedral sites in quartz at four pressures up to 10.2 GPa using the data of Glinnemann et al. (1992). We define the intrafacial angle variance from a regular tetrahedron as $\sigma_{\text{OR}}^2 = \sum_{i=1,12}(\theta_i - 60^\circ)^2/12$ and from a Sommerville tetrahedron as $\sigma_{\text{OS}}^2 = \sum_{i=1,4}(\theta_i - 70.53^\circ)^2/12 + \sum_{j=1,8}(\theta_j - 54.74^\circ)^2/12$. Intrafacial angle variance was chosen over tetrahedral angle variance (Robinson et al. 1971) to avoid dependence on fictive cations in the unoccupied sites. However, placing fictive cations at the centroids of the unoccupied sites and calculating tetrahedral angle variance produces parallel trends. Figure 5a shows the change in angle variance with pressure for the silica tetrahedron. It becomes more distorted compared to regular tetrahedra and less distorted from Sommerville tetrahedra. Figure 5b illustrates the average change in angle variance with pressure for the seven unoccupied tetrahedra. Distortion from both Sommerville and from perfectly regular tetrahedra decreases as pressure increases. This is because the unoccupied tetrahedra, while more like Sommerville than regular, are so distorted from both that measures of distortion from Sommerville and regular

can decrease simultaneously. These two parameters show that the silica tetrahedron trends toward a BCC Sommerville tetrahedron with pressure, but the unoccupied tetrahedra are so distorted that it is only possible to say that the unoccupied tetrahedra are more like Sommerville tetrahedra than regular tetrahedra over this pressure domain. This obscures the fact that the decrease in distortion from Sommerville tetrahedra reflects the underlying process, but the decrease in distortion from regular tetrahedra is an artifact of the extreme initial distortion of the tetrahedra. Consistent with this, it is theoretically possible for the tetrahedra to become perfectly Sommerville if observed trends continue, but not perfectly regular, because it is impossible to completely fill space using only regular tetrahedra (Sommerville 1923a, 1923b).

Figure 5 shows that the change in the distortion in the unoccupied tetrahedra with pressure is much greater than in the silicate tetrahedron, and Figure 6 shows that the volumes of the unoccupied tetrahedra decrease much more than the volume of the occupied tetrahedron, which is nearly constant over 10.2 GPa. Thus, most of the action in quartz as it is compressed is in the unoccupied tetrahedra. Near neighbor anion-anion distances (Fig. 7) were calculated for quartz up to 10.2 GPa using the data of Glinnemann et al. (1992). Each anion bridges two tetrahedra and has six intra-silicate tetrahedron near neighbor anions, three from one tetrahedron, and three from another. Figure 7 plots the average of these distances [$\langle R(\text{O-O}) \rangle$], which remains essentially unchanged with pressure, and the individual distances to the next six closest anions. Among these six, there are two pairs of symmetrically equivalent distances, resulting in four curves representing six distances. These distances are short enough that it is reasonable to hypothesize that the anions interact in a nonbonded closed-shell manner, i.e., via electrostatic repulsion, especially in light of the fact that considerable electron density must be tied up in the short, strong Si-O bonds, reducing nuclear shielding. Anions that interact repulsively orient themselves so as to maximize their minimum near neighbor distances. This drives them toward the least dense regular packing that the ratio of the number of anions to volume allows, in this case BCC. As pressure forces the anions together, they interact repulsively with their inter-tetrahedral near neighbors, to the extent that the very

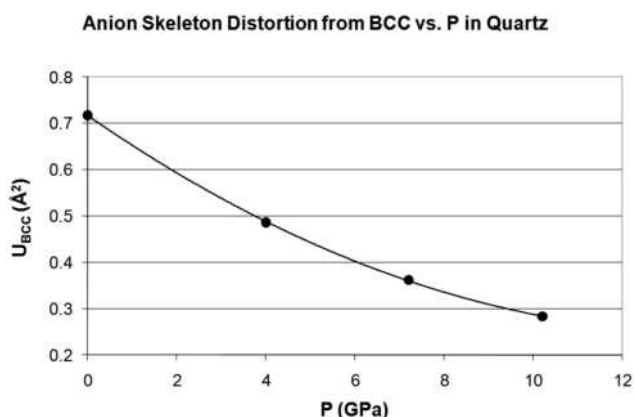


FIGURE 4. U_{BCC} quantifies the distortion of the anion skeleton of quartz from ideal BCC. The anion skeleton of quartz moves dramatically toward BCC with pressure.

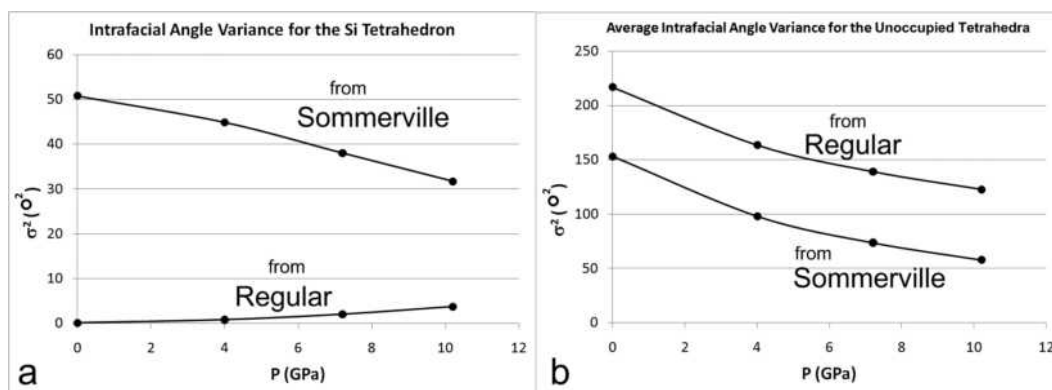


FIGURE 5. Intrafacial angle variance for all of the tetrahedral sites in quartz at four pressures up to 10.2 GPa calculated using the data of Glinnemann et al. (1992). Figure a shows the variance of the silica tetrahedron from both a Sommerville and a regular tetrahedron. Figure b shows the average of these values for the seven unoccupied tetrahedral sites.

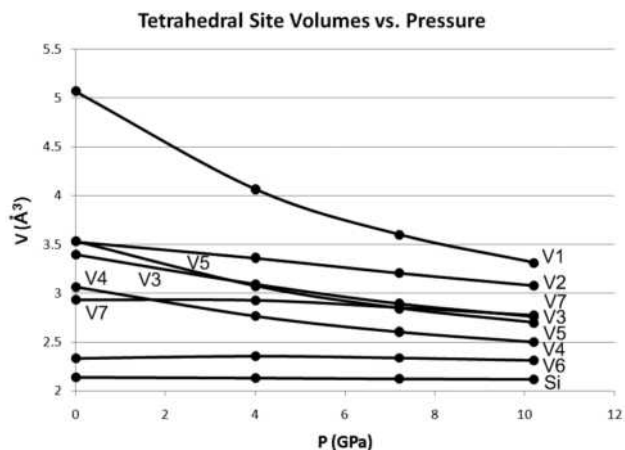


FIGURE 6. The volume of the eight nonequivalent tetrahedral sites in quartz at four pressures up to 10.2 GPa calculated using the data of Glinnemann et al. (1992). This plot demonstrates that most of the action in quartz as it is compressed is happening in the unoccupied sites.

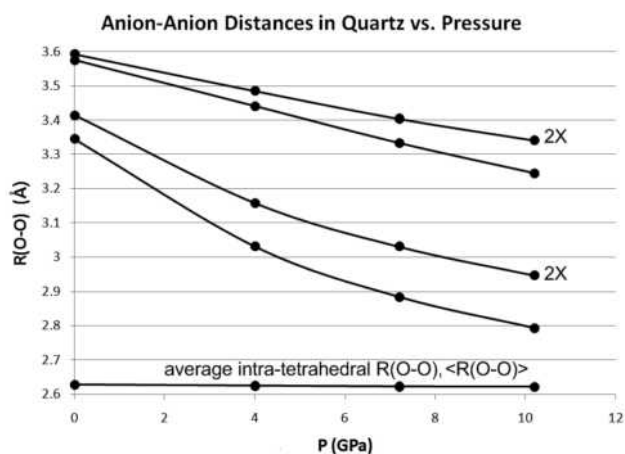


FIGURE 7. A comparison over 10.2 GPa (Glinnemann et al. 1992) of the average of the distances, $\langle R(O-O) \rangle$, between the O atom in quartz and its six intra-tetrahedral near neighbor anions, and the individual distances to the next six closest anions.

stable $(SiO_4)^+$ groups distort away from regular tetrahedra toward BCC Sommerville tetrahedra. Thus, tetrahedral distortion is not a compression mechanism according to the definition of the introduction (i.e., because it is not helping to reduce volume), rather a result of anion-anion interaction. This is further evidenced by the fact that the silica tetrahedral volume in quartz decreases by $<1\%$ over 10.2 GPa, but the volume of the bulk structure decreases by almost 16% (Glinnemann et al. 1992).

COMPARISON OF THE COMPRESSIBILITIES OF QUARTZ, CRISTOBALITE, AND COESITE

Figure 8 is a plot reprinted from Prewitt and Downs (1998), itself modified from Downs and Palmer (1994), showing the fractional change in Si-O-Si angle with change in volume for quartz, coesite, and cristobalite (Glinnemann et al. 1992; Levien et al. 1980; Levien and Prewitt 1981; Downs and Palmer 1994; Hazen et al. 1989). The data points define an almost perfect straight line, demonstrating that compression in the tetrahedral

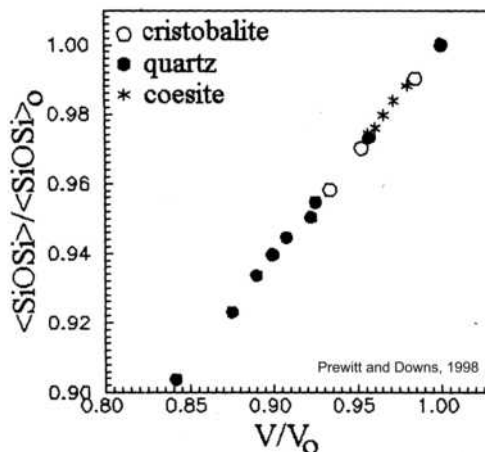


FIGURE 8. A plot reprinted from Prewitt and Downs (1998) showing that Si-O-Si angle-bending controls compression in the tetrahedral silica polymorphs.

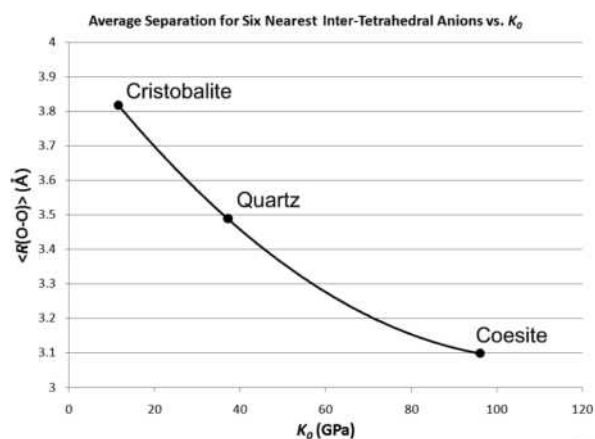


FIGURE 9. A plot of the average O-O separation for the six nearest anions that do not share a coordinating silicon in cristobalite (Downs and Palmer 1994), quartz (Glinnemann et al. 1992), and coesite (Angel et al. 2003).

silica polymorphs is correlated with Si-O-Si angle-bending. However, the bulk moduli of cristobalite, quartz, and coesite differ dramatically: 11.5, 37.1, and 96 GPa, respectively (Downs and Palmer 1994; Levien et al. 1980; Levien and Prewitt 1981). This is because the change in Si-O-Si angle per unit pressure varies correspondingly: $6^\circ/\text{GPa}$ in cristobalite, $1.4^\circ/\text{GPa}$ in quartz, $0.6^\circ/\text{GPa}$ in coesite. That is, a given reduction in Si-O-Si angle creates the same volume reduction in quartz as in cristobalite and coesite, but it requires four times more pressure to reduce the angle in quartz than it does in cristobalite, and more than twice as much in coesite as in quartz. We have put forth the hypothesis that anion-anion repulsive interaction in quartz resists compression. Figure 9 shows the average O-O separation for the six nearest inter-silica tetrahedron neighbor anions (i.e., anions that do not share a coordinating silicon) in cristobalite, quartz, and coesite (Downs and Palmer 1994; Angel et al. 2003; Levien and Prewitt 1981). The non-Si sharing nearest neighbor anions are significantly farther away in cristobalite than they are in quartz, 3.82 vs.

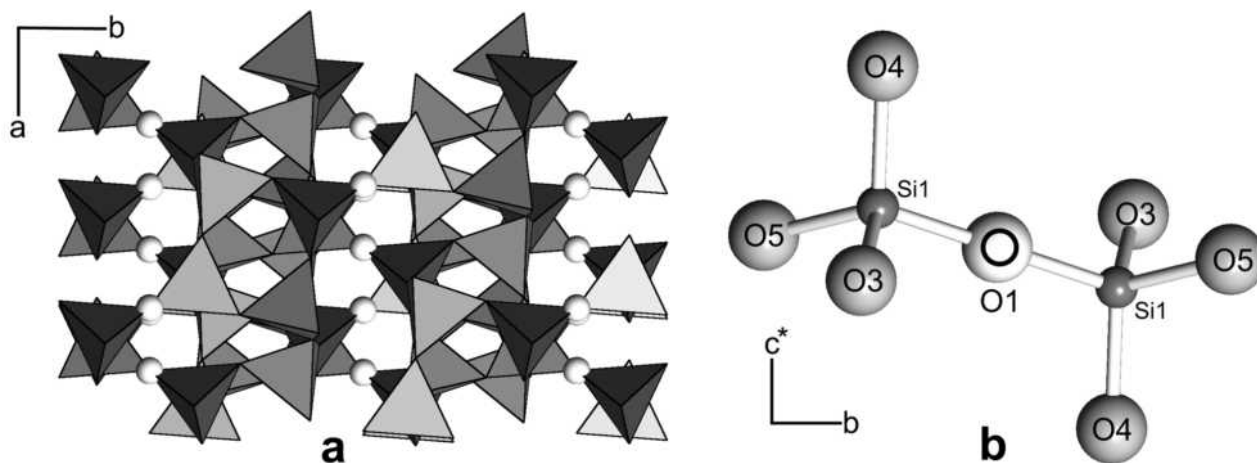


FIGURE 10. The unusual 180° Si1-O1-Si1 angle in coesite (Angel et al. 2003). O1 is on an inversion center.

3.49 Å, and are much closer in coesite, 3.10 Å, consistent with our hypothesis that inter-tetrahedral anions interact repulsively, so that the closer they are, the stiffer the structure.

There is an additional mechanism that stiffens the average Si-O-Si angle in coesite. Cristobalite and quartz have only one O atom in their asymmetric units, so there is only one crystallographically unique Si-O-Si angle, but the unit cell of coesite has five nonequivalent O atoms, so there are five different Si-O-Si angles that can behave differently. O1 lies on an inversion center, so as long as the forces inside coesite maintain this symmetry as pressure increases, then the Si1-O1-Si1 angle is constrained to the unusual value 180° , as illustrated in Figure 10b. Figure 10a shows a portion of the bulk structure of coesite with O1 illustrated as a sphere, emphasizing the importance of the Si1-O1-Si1 angle. Recent work (Angel et al. 2003) concludes that the Si1-O1-Si1 angle is 180° , that it does not change with pressure, and that it is not an average value due to toroidal motion about an Si1-Si1 axis. Therefore, all angle-bending must occur at the other four Si-O-Si angles, reducing the decrease in $\langle \text{Si-O-Si} \rangle$ per unit pressure.

Because quartz is based on BCC packing of anions, it is the perfect material to analyze for evidence of anion-anion interactions, per the following explanation. In materials based on closest packing of anions, such as olivines or pyroxenes, volume reduction considerations and anion-anion repulsion both tend to make polyhedra more regular with pressure. This is because ideal closest-packed arrangements have perfectly regular tetrahedra and octahedra, and regular polyhedra are not only the most volume-efficient, but also maximize the minimum anion-anion distance (in the closest-packed case). This means that in closest-packed materials, the effects of volume reduction considerations and anion-anion repulsion cannot be distinguished on the basis of polyhedral behavior with pressure. However, in a BCC arrangement, volume-reduction considerations still favor regular polyhedra, but maximizing the minimum anion-anion distance favors Sommerville tetrahedra. In this case, volume reduction and anion-anion repulsion have competing, different effects on polyhedral behavior with pressure, and can therefore be distinguished. In quartz, the only significant compression

mechanism is Si-O-Si angle-bending, anion-anion repulsion is an “anti-compression” mechanism, stiffening the structure relative to cristobalite, and tetrahedral morphology is responding to anion-anion repulsive interaction.

Finally, a stabilizing bonded interaction between anions may play a role in the movement of the anions in quartz toward BCC with pressure. Properties of some O-O bond paths in silicates as determined by *ab initio* calculations suggest that these are stabilizing interactions (Gibbs et al. 2008). Calculations by Gibbs et al. (1999) showed a bond path forming between two of the anions in adjacent Si-tetrahedra in quartz above 2.5 GPa. This bond path is between O atoms that are BCC nearest neighbors, perhaps locally stabilizing the BCC arrangement and facilitating the move toward ideal BCC.

ACKNOWLEDGMENTS

We thank G.V. Gibbs and two anonymous referees for their valuable suggestions. We also thank Associate Editor E.S. Grew who went above and beyond. The careful editing of these four colleagues has dramatically improved our paper.

REFERENCES CITED

- Angel, R.J., Shaw, C.S.J., and Gibbs, G.V. (2003) Compression mechanisms of coesite. *Physics and Chemistry of Minerals*, 30, 167–176.
- Bragg, S.L., Claringbull, G.F., and Taylor, W.H. (1965) *Crystal Structures of Minerals*, 409 p. Cornell University Press, Ithaca, New York.
- Cohen, R.E. (1994) First-principles theory of crystalline SiO_2 . In P.J. Heaney, C.T. Prewitt, and G.V. Gibbs, Eds., *Silica, Physical Behavior, Geochemistry, and Materials Applications*, 29, p. 275–382. Reviews in Mineralogy, Mineralogical Society of America, Chantilly, Virginia.
- d'Amour, H., Denner, W., and Schulz, H. (1979) Structure determination of α -quartz up to 68×10^8 Pa. *Acta Crystallographica*, B35, 550–555.
- Deer, W.A., Howie, R.A., and Zussman, J. (1978) *Rock-Forming Minerals, Volume 2A, Single Chain Silicates*, 2nd edition, 668 p. Wiley, New York.
- Downs, R.T. and Palmer, D.C. (1994) The pressure behavior of α cristobalite. *American Mineralogist*, 79, 9–14.
- Gibbs, G.V., Rosso, K.M., Teter, D.M., Boisen Jr., M.B., and Bukowinski, M.S.T. (1999) Model structures and properties of the electron density distribution for low quartz at pressure: a study of the SiO bond. *Journal of Molecular Structures*, 485–486, 13–25.
- Gibbs, G.V., Downs, R.T., Cox, D.F., Ross, N.L., Boisen Jr., M.B., and Rosso, K.M. (2008) Shared and closed-shell O-O interactions in silicates. *Journal of Physical Chemistry*, A112, 3693–3699.
- Glinnemann, J., King Jr., H.E., Schulz, H., Hahn, Th., La Placa, S.J., and Dacol, F. (1992) Crystal structures of the low-temperature quartz-type phases of SiO_2 and GeO_2 at elevated pressure. *Zeitschrift für Kristallographie*, 198, 177–212.
- Haines, J., Léger, J.M., Gorelli, F., and Hanfland, M. (2001) Crystalline post-quartz phase in silica at high pressure. *Physical Review Letters*, 87, 155503.

- Hazen, R.M. (1999) Crystal compression revisited: Role of second-order effects. EOS Transactions, AGU, Fall Meeting Supplement, 80 (46), F1139.
- Hazen, R.M. and Finger, L.W. (1982) Comparative Crystal Chemistry, 231 p. Wiley, New York.
- Hazen, R.M., Finger, L.W., Hemley, R.J., and Mao, H.K. (1989) High-pressure crystal chemistry and amorphization of α -quartz. Solid State Communications, 72, 507–511.
- Jorgensen, J.D. (1978) Compression mechanisms in α -quartz structures—SiO₂ and GeO₂. Journal of Applied Physics, 49, 5473–5478.
- Kim-Zajonz, J., Werner, S., and Schulz, H. (1999) High pressure single crystal X-ray diffraction study on α -quartz. Zeitschrift für Kristallographie, 214, 324–330.
- Levien, L. and Prewitt, C.T. (1981) High-pressure crystal structure and compressibility of coesite. American Mineralogist, 66, 324–333.
- Levien, L., Prewitt, C.T., and Weidner, D.J. (1980) Structure and elastic properties of quartz at pressure. American Mineralogist, 65, 920–930.
- McCarthy, A.C., Downs, R.T., and Thompson, R.M. (2008) Compressibility trends of the clinopyroxenes, and an in-situ high-pressure single-crystal X-ray diffraction study of jadeite. American Mineralogist, 93, 198–209.
- Nestola, F., Boffa Ballaran, T., Liebske, C., Thompson, R.M., and Downs, R.T. (2008) The effect of the hedenbergitic substitution on the compressibility of jadeite. American Mineralogist, 93, 1005–1013.
- Ogata, K., Takéuchi, Y., and Kudoh, Y. (1987) Structure of α -quartz as a function of temperature and pressure. Zeitschrift für Kristallographie, 179, 403–413.
- O'Keeffe, M. and Hyde, B.G. (1996) Crystal Structures, Volume 1, 453 p. Mineralogical Society of America Monograph 2, Chantilly, Virginia.
- Origlieri, M., Downs, R.T., Thompson, R.M., Pommier, C.J.S., Denton, M.B., and Harlow, G.E. (2003) High-pressure crystal structure of kosmochlor, NaCrSi₂O₆ and systematics of anisotropic compression of pyroxenes. American Mineralogist, 88, 1025–1032.
- Pauling, L. (1940) Nature of the Chemical Bond, 450 p. Cornell University Press, Ithaca, New York.
- Prencipe, M. and Nestola, F. (2007) Minerals at high pressure. Mechanics of compression from quantum mechanical calculations in a case study: The beryl (Al₄Be₆Si₁₂O₃₆). Physics and Chemistry of Minerals, 34, 37–52.
- Prewitt, C.T. and Downs, R.T. (1998) High-pressure crystal chemistry. In R.J. Hemley, Eds., Ultrahigh-Pressure Mineralogy: Physics and Chemistry of the Earth's Deep Interior, 37, p. 283–317. Reviews in Mineralogy, Mineralogical Society of America, Chantilly, Virginia.
- Robinson, K., Gibbs, G.V., and Ribbe, P.H. (1971) Quadratic elongation: A quantitative measure of distortion in coordination polyhedra. Science, 172, 567–570.
- Ross, N.L. (2000) Framework structures. In R.M. Hazen and R.T. Downs, Eds., High-Temperature and High-Pressure Crystal Chemistry, 41, p. 257–287. Reviews in Mineralogy, Mineralogical Society of America, Chantilly, Virginia.
- Sommerville, D.M.Y. (1923a) Division of space by congruent triangles and tetrahedra. Proceedings of the Royal Society of Edinburgh, 43, 85–116.
- (1923b) Space filling tetrahedra in Euclidean space. Proceedings of the Edinburgh Mathematical Society, 41, 49–57.
- Sowa, H. (1988) The O packings of low-quartz and ReO₃ under high pressure. Zeitschrift für Kristallographie, 184, 257–268.
- Taylor, S.R. and McLennan, S.M. (1985) The Continental Crust: Its Composition and Evolution, 312 p. Blackwell Scientific Publications, Oxford.
- Thompson, R.M. and Downs, R.T. (2001a) Quantifying distortion from ideal closest-packing in a crystal structure with analysis and application. Acta Crystallographica, B57, 119–127.
- (2001b) Systematic generation of all nonequivalent closest-packed stacking sequences of length N using group theory. Acta Crystallographica, B57, 766–771.
- (2003) Model pyroxenes I: Ideal pyroxene topologies. American Mineralogist, 88, 653–666.
- (2004) Model pyroxenes II: Structural variation as a function of tetrahedral rotation. American Mineralogist, 89, 614–628.
- (2008) The crystal structure of diopside at pressure to 10 GPa. American Mineralogist, 93, 177–186.
- Thompson, R.M., Downs, R.T., and Redhammer, G.T. (2005) Model pyroxenes III: Volume of C2/c pyroxenes at mantle P, T, and x. American Mineralogist, 90, 1840–1851.

MANUSCRIPT RECEIVED MARCH 13, 2009

MANUSCRIPT ACCEPTED SEPTEMBER 10, 2009

MANUSCRIPT HANDLED BY EDWARD GREW